

Determination of Reactive Properties of a Series of Mono-Functionalized Bis-tetrathiafulvalene Employing DFT Calculations

Amel Bendjeddou^{a*}, Tahar Abbas^b, Abdelkrim Gouasmia^c, Didier Villemin^d

^{a,b}Laboratory of Aquatic and Terrestrial Ecosystems, Org. and Bioorg. Chem. Group, University of Mohamed-Cherif Messaadia, Souk Ahras, 41000, Algeria

^cLaboratory of Organic Materials and Heterochemistry, University of Larbi Tebessi, Tebessa, 12000, Algeria

^dLaboratory of Molecular and Thio-Organic Chemistry, UMR CNRS 6507, INC3M, FR 3038, Labex EMC3, ensicaen & University of Caen, Caen 14050, France

^{a,b}Email: amel.bendjeddou@univ-soukahras.dz; tahar.abbaz@univ-soukahras.dz

^cEmail: akgouasmia@hotmail.com

^dEmail: didier.villemin@ensicaen.fr

Abstract

Density functional Theory (DFT) calculations at the B3LYP/6-31G (d,p) level of theory are carried out to investigate the equilibrium geometry of the novel compounds **3(a-e)**. Moreover, The Molecular electrostatic Potential (MEP) analysis reveals the sites for electrophilic attack and nucleophilic reactions within the molecules. Additionally, the reactivity and reactive site within the mono-functionalized bis-tetrathiafulvalenes, dipole moment, theoretical study of the electronic structure, nonlinear optical properties (NLO), and natural bonding orbital (NBO) analysis are performed and discussed.

Keywords: Tetrathiafulvalenes; density functional theory; computational chemistry; electronic structure; quantum chemical calculations.

* Corresponding author.

1. Introduction

Tetrathiafulvalene (TTF) chemistry has a long history since the first discovery of its conductivity within the Nineteen Seventies [1,2]. Interests within the related molecules have spread into varied fields concerned with electroactive materials due to their potential for the electronic devices like field effect transistors (FETs) [3,4], and photovoltaic cells [5,6]. Carrier generation is the primary concern in order to obtain electroactive organic materials. The carriers in molecular conductors [7,8] are usually generated based on a charge-transfer mechanism between the electron donor and acceptor molecules, a mechanism that was proposed by Mulliken within the Fifties [9]. This mechanism is the underlying conception for carrier generation within the current molecular conductors, and thereafter has been extensively adopted for single-component molecular conductors [10]. Intensive search for interesting and promising organic materials to indicate highly conducting or even superconducting properties, unique magnetic ordering or interesting optical characteristics has resulted within the synthesis of new electron donor and acceptor molecules. An enormous majority of organic metal-like materials is derived of tetrathiafulvalene (TTF) including its symmetrical and unsymmetrical derivatives. By means of increasing development of computational chemistry within the past decade, the research of theoretical modeling of drug design, functional material design, etc., has become much more mature than ever. Several important physico-chemical properties of biological and chemical systems can be predicted from the first principles by varied computational techniques [11]. In recent years, density functional theory (DFT) has been a shooting star in theoretical modeling. the development of higher and better exchange-correlation functionals made it possible to calculate several molecular properties with comparable accuracies to traditional correlated ab initio ways, with a lot of favorable computational costs [12]. Literature survey disclosed that the DFT has a great accuracy in reproducing the experimental values of in geometry, dipole moment, vibrational frequency, etc. [13,14]. In recent years organic nonlinear optical (NLO) materials have attracted attention, due to their second or third order hyper-polarizabilities compared to those of inorganic NLO materials [15]. Several studies are being carried out to synthesize new organic materials with large second-order optical nonlinear property in order to satisfy present and future technological needs [16]. They find innumerable applications within the various fields like telecommunications, optical computing, and optical data storage. In the present work the geometrical parameters, Natural Bond Orbital (NBO) analysis and electrostatic potential were calculated using B3LYP method with 6-31G (d,p) as basis set. The electronic dipole moment (μ) and first order hyperpolarizability (β) value of the molecules are computed to study the Non-Linear Optical (NLO) property. NBO analyses were performed to provide valuable information regarding various intermolecular interactions. The calculated Highest Occupied Molecular Orbital (HOMO) and Lowest Unoccupied Molecular Orbital (LUMO) energies show that charge transfer occurs within the molecules. Finally electronegativity (χ), hardness (η), softness (S) and Molecular electrostatic Potential maps (MEP) properties were calculated.

2. Materials and methods

All the quantum chemical calculations have been carried out with Gaussian 09 program package to predict the molecular structure, NBO, NLO and energy of the optimized structures using B3LYP functional and 6-31G (d,p) basis set, which invokes Becke's three parameter hybrid exchange functional (B3), with Lee-Yang-Parr correlational functional (LYP). The basis set 6-31G (d,p) with 'd' polarization functions on heavy atoms and 'p'

polarization functions on hydrogen atoms are used for better description of polar bonds of molecule.

3. Results and discussion

3.1. Chemistry

In a precedent work [17], we have explained the synthesis of bis-tetrathiafulvalenes indicated in Figure 4. The synthetic route used to lead to the target functional linker between TTF units, is based on the reaction between two different functions respectively attached to a specific TTF ring. To incorporate an ester function in a link between TTF units, a reaction involving an acid chloride function of a TTF and one hydroxyl group of another TTF ring was used. As shown in Figure 4, the use of monohydroxyTTF **2** [18-20] with 1.5 equiv. of acid chloride TTF **1** [21-23] led to a series of mono-functionalized bisTTF **3(a-e)**.

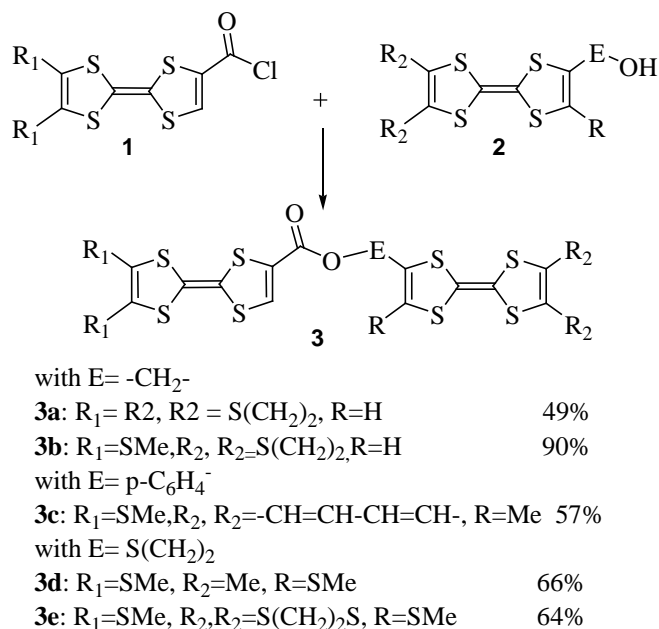


Figure 4: Synthetic route for the preparation of mono-functionalized bisTTF **3(a-e)**

3.2. Molecular geometry

The optimized DFT geometries by B3LYP/6-31G (d,p) of the bis-TTF with atom numbering are shown in Figure 1. The internal coordinates describe the position of the atoms in terms of distances, angles and dihedral angles with respect to an origin atom.

The symmetry coordinates are constructed using the set of internal coordinates. In this study, the standard internal coordinates for compounds **3(a-e)** are presented in Tables 1-5. By allowing the relaxation of all parameters, the calculations converge to optimized geometries, which correspond to true energy minima, as revealed by the lack of imaginary frequencies in the vibrational mode calculation.

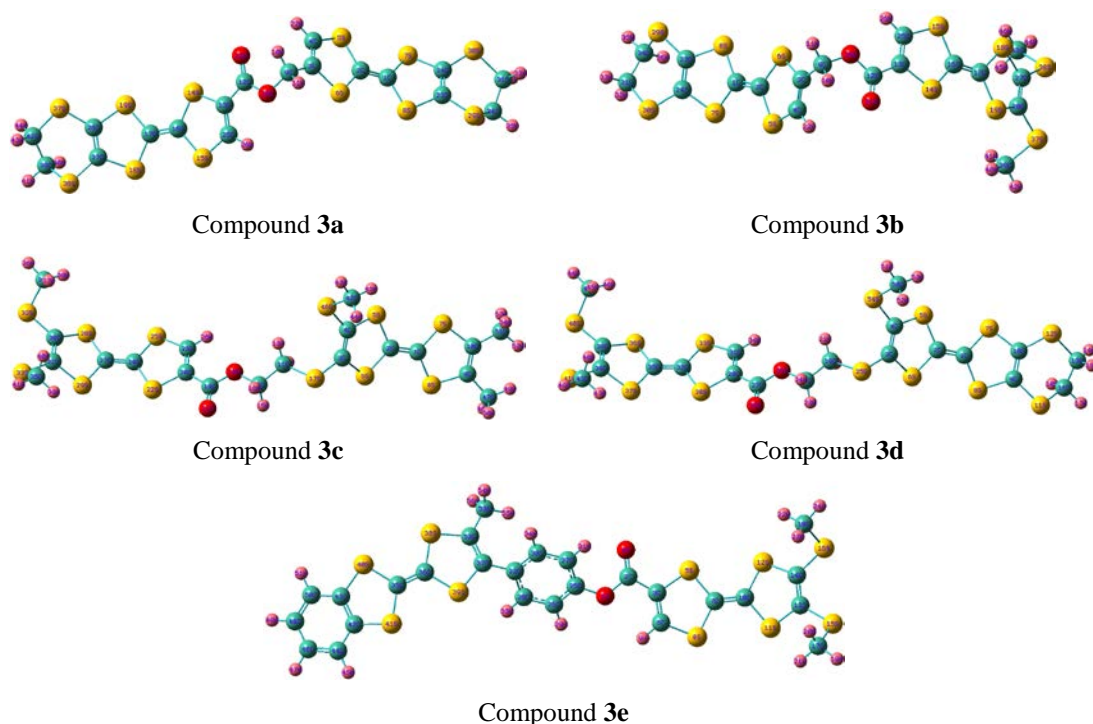


Figure 1: Optimized molecular structure of mono-functionalized bisTTF **3(a-e)**

Table 1: Optimized geometric parameters of compound **3a**

Bond Length(Å)		Bond Angles (°)		Dihedral Angles (°)	
R(1,2)	1.350	A(2,1,7)	123.507	D(7,1,2,6)	178.288
R(1,7)	1.783	A(2,1,8)	123.849	D(2,1,7,24)	156.897
R(1,8)	1.781	A(7,1,8)	112.629	D(1,2,6,3)	169.553
R(2,5)	1.787	A(1,2,5)	123.142	D(6,3,4,22)	176.171
R(2,6)	1.782	A(1,2,6)	123.289	D(4,3,9,20)	102.355
R(3,4)	1.341	A(5,2,6)	113.563	D(6,3,9,10)	164.044
R(3,6)	1.779	A(13,12,20)	112.058	D(22,4,5,2)	176.572
R(3,9)	1.499	A(13,12,21)	123.526	D(1,8,23,29)	173.077
R(9,20)	1.452	A(20,12,21)	124.415	D(11,9,20,12)	153.158
R(12,13)	1.473	A(24,23,29)	123.841	D(20,12,13,14)	178.571
R(12,20)	1.356	A(7,24,30)	115.375	D(21,12,13,25)	175.893
R(12,21)	1.216	A(23,29,34)	96.395	D(13,12,20,9)	177.213
R(30,31)	1.862	A(24,30,31)	103.831	D(14,13,25,26)	177.544
R(31,32)	1.095	A(29,34,31)	113.017	D(13,14,16,17)	169.103
R(31,33)	1.092	A(37,42,44)	105.867	D(14,16,17,18)	178.211

Table 2: Optimized geometric parameters of compound **3b**

	Bond Length(Å)	Bond Angles (°)	Dihedral Angles (°)		
R(1,2)	1.350	A(2,1,7)	123.526	D(7,1,2,5)	178.206
R(1,7)	1.783	A(2,1,8)	123.825	D(8,1,2,6)	156.955
R(1,8)	1.781	A(7,1,8)	112.633	D(6,2,5,4)	169.559
R(2,5)	1.787	A(1,2,5)	123.145	D(6,3,4,5)	176.224
R(2,6)	1.782	A(1,2,6)	123.293	D(4,3,9,11)	102.788
R(3,4)	1.341	A(5,2,6)	113.557	D(4,3,9,20)	164.498
R(3,6)	1.779	A(4,3,6)	116.574	D(3,4,5,2)	176.518
R(3,9)	1.499	A(4,3,9)	124.739	D(1,8,23,24)	172.973
R(9,10)	1.091	A(2,5,4)	94.687	D(10,9,20,12)	152.630
R(12,13)	1.472	A(2,6,3)	94.966	D(11,9,20,12)	177.370
R(12,20)	1.356	A(1,7,24)	93.592	D(21,12,13,25)	177.806
R(12,21)	1.216	A(1,8,23)	93.508	D(21,12,20,9)	175.362
R(13,25)	1.347	A(20,12,21)	124.397	D(25,13,14,16)	177.882
R(38,43)	1.837	A(28,37,39)	101.790	D(25,15,16,14)	169.738
R(39,40)	1.091	A(27,38,43)	101.648	D(15,16,17,18)	179.590

Table 3: Optimized geometric parameters of compound **3c**

	Bond Length(Å)	Bond Angles (°)	Dihedral Angles (°)		
R(1,2)	1.350	A(2,1,7)	123.474	D(7,1,2,6)	179.255
R(1,7)	1.777	A(2,1,8)	123.451	D(2,1,7,10)	168.988
R(1,8)	1.777	A(7,1,8)	113.066	D(1,2,6,3)	160.155
R(2,5)	1.782	A(1,2,5)	123.839	D(6,3,4,46)	175.432
R(2,6)	1.784	A(1,2,6)	123.881	D(46,4,5,2)	171.541
R(3,4)	1.355	A(5,2,6)	112.274	D(3,4,46,42)	114.963
R(3,6)	1.781	A(12,11,13)	110.436	D(1,8,9,47)	173.541
R(3,17)	1.773	A(3,17,11)	101.290	D(47,9,10,7)	178.861
R(9,10)	1.345	A(18,19,20)	112.210	D(8,9,47,49)	174.507
R(18,19)	1.354	A(27,28,30)	94.526	D(10,9,47,50)	116.193
R(19,21)	1.215	A(27,29,31)	94.517	D(9,10,51,53)	124.011
R(23,26)	1.083	A(31,30,32)	125.697	D(13,11,12,15)	177.096
R(27,28)	1.779	A(30,32,34)	101.727	D(14,11,12,16)	177.404
R(27,29)	1.779	A(31,33,35)	101.807	D(17,11,12,18)	177.534
R(30,32)	1.766	A(32,34,37)	110.713	D(12,11,17,3)	165.179

Table 4: Optimized geometric parameters of compound **3d**

	Bond Length(Å)	Bond Angles (°)	Dihedral Angles (°)		
R(1,2)	1.350	A(2,1,7)	123.430	D(7,1,2,6)	178.119
R(1,7)	1.783	A(2,1,8)	123.764	D(2,1,7,10)	158.535
R(1,8)	1.781	A(7,1,8)	112.773	D(1,2,6,3)	162.733
R(2,5)	1.781	A(1,2,5)	123.745	D(6,3,4,54)	175.459
R(2,6)	1.782	A(1,2,6)	123.723	D(54,4,5,2)	172.543
R(3,4)	1.355	A(5,2,6)	112.507	D(3,4,54,50)	115.052
R(3,6)	1.781	A(4,3,6)	117.056	D(1,8,9,11)	173.449
R(3,25)	1.773	A(1,8,9)	93.615	D(11,9,10,7)	171.756
R(9,10)	1.350	A(9,11,16)	96.355	D(7,10,12,13)	150.808
R(9,11)	1.763	A(10,12,13)	103.807	D(10,12,13,14)	127.959
R(10,12)	1.764	A(11,16,18)	107.939	D(21,19,20,23)	176.699
R(16,17)	1.094	A(17,16,18)	108.596	D(22,19,20,24)	177.055
R(26,27)	1.354	A(26,27,29)	124.093	D(25,19,20,26)	177.093
R(27,28)	1.474	A(38,40,42)	101.699	D(20,19,25,3)	163.877
R(27,29)	1.215	A(39,41,43)	101.844	D(19,20,26,27)	179.965

Table 5: Optimized geometric parameters of compound **3e**

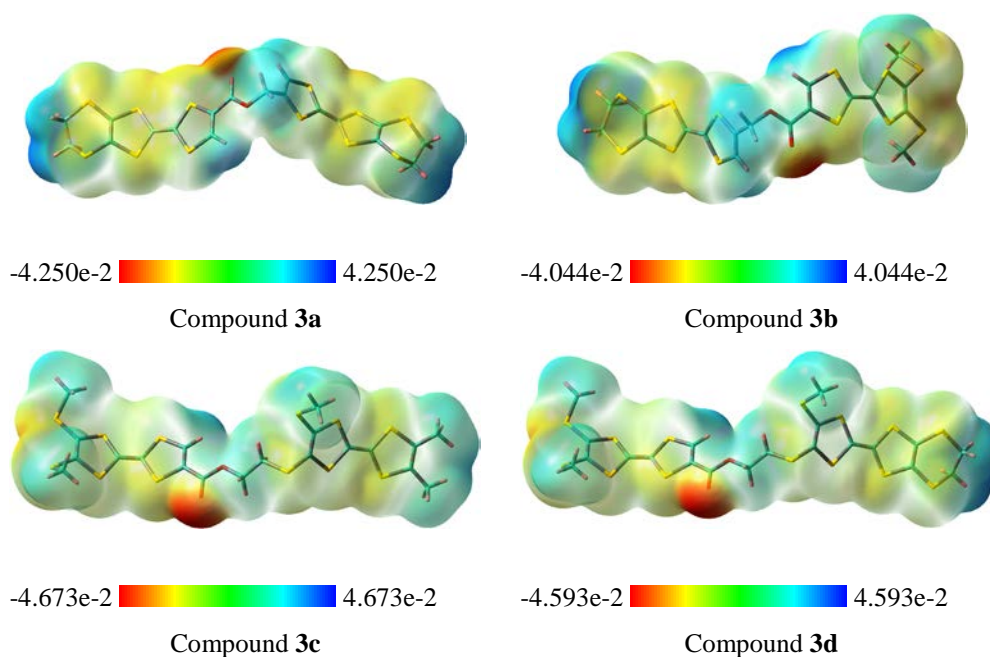
	Bond Length(Å)	Bond Angles (°)	Dihedral Angles (°)		
R(1,2)	1.368	A(2,1,25)	121.362	D(2,1,25,26)	141.099
R(1,25)	1.395	A(1,2,3)	110.943	D(1,2,3,5)	179.069
R(2,3)	1.472	A(1,2,4)	125.252	D(2,3,5,7)	175.122
R(2,4)	1.211	A(3,2,4)	123.805	D(2,3,6,8)	177.935
R(3,5)	1.776	A(2,3,5)	116.115	D(10,7,8,6)	169.580
R(3,6)	1.348	A(2,3,6)	126.269	D(8,7,10,12)	179.438
R(5,7)	1.785	A(10,11,13)	94.596	D(7,10,12,14)	158.762
R(6,8)	1.741	A(10,12,14)	94.604	D(10,11,13,15)	172.487
R(6,9)	1.083	A(13,15,17)	101.738	D(15,13,14,12)	172.903
R(7,10)	1.349	A(14,16,18)	101.877	D(14,13,15,17)	123.319
R(18,22)	1.091	A(1,25,27)	123.281	D(13,15,17,19)	177.341
R(42,43)	1.404	A(26,25,27)	120.991	D(1,25,26,28)	176.411
R(44,45)	1.086	A(28,26,29)	121.114	D(26,25,27,31)	179.216
R(46,48)	1.396	A(42,44,46)	119.408	D(25,26,28,33)	179.446
R(48,49)	1.085	A(54,53,56)	107.304	D(25,27,30,34)	178.127

3.3. Molecular electrostatic potential

The molecular electrostatic potential $V(r)$ that is created in the space around a molecule by its nuclei and electrons is well established as a guide to molecular reactive behavior. It is defined by:

$$V(r) = \sum Z_A / |R_A - r| - \int \rho(r') / |r' - r| d^3r'$$

In which Z_A is the charge of nucleus A, located at R_A , $\rho(r')$ is the electronic density function for the molecule and r' is the dummy integration variable [24,25]. MEP is related to the electronic density and is a very useful descriptor in determining sites for electrophilic and nucleophilic reactions as well as hydrogen bonding interactions [26,27]. Being a real physical property, $V(r)$ can be determined experimentally by diffraction or by computational methods [28]. However, identification of reactivity patterns based on the MEP exhibits intrinsic drawbacks, since the MEP is obtained through the classical electrostatic potential [29]. Then it is not possible to determine sites for nucleophilic attack because the zones of positive potential are not necessarily expressing affinity for nucleophiles but the concentrated nature of the nuclear charges. Molecular electrostatic potential mapping is very useful in the investigation of the molecular structure with its physiochemical property relationships [30-32]. The MEP map of bis-TTF **3(a-e)** visibly suggests that the region around carbon atoms linked through double bond with oxygen atom represents the most negative potential region (red). The hydrogen atoms attached to the ends of the molecular chain bear the maximum bang of positive charge (blue). The color scheme for MEP surface is red, electron rich, partially negative charge; blue, electron deficient, partially positive charge; light blue, slightly electron deficient region; yellow, slightly electron rich region, respectively. The negative (red) region of MEP was related to electrophilic reactivity and the positive (blue) region to nucleophilic reactivity (Figure 2).



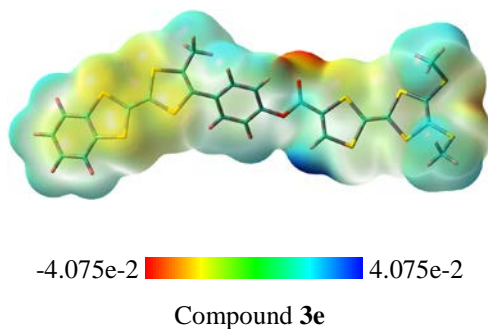


Figure 2: Molecular electrostatic potential surface of mono-functionalized bisTTF **3(a-e)**

3.4. Frontier molecular orbitals (FMOs)

The frontier molecular orbitals can offer a reasonable qualitative prediction of the excitation properties and the ability of electron transport [33,34]. The electronic absorption basically means the transition from the ground to the first excited state and is mainly described by one electron transition from the highest occupied molecular orbital (HOMO) to the lowest unoccupied molecular orbital (LUMO). In other words, HOMO is the orbital that acts as an electron donor whereas LUMO is an orbital that acts as electron acceptor. The energy values of HOMO and LUMO and their energy gap reflect the chemical activity of the molecules. Figure 3 show the distributions and energy levels of the HOMO-1, HOMO, LUMO and LUMO+1 orbitals computed at the B3LYP/6-31G (d,p) level for compound **3c**.

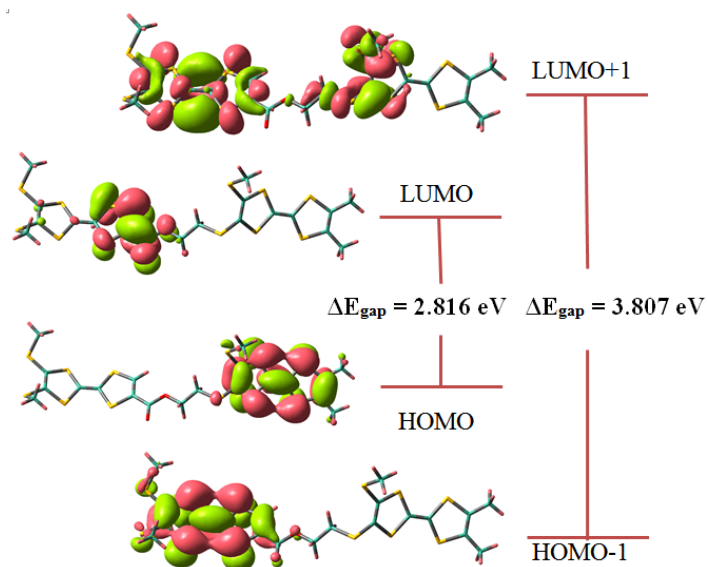


Figure 3: HOMO-LUMO Structure with the energy level diagram of compound **3c**

3.5. Global reactivity descriptors

Global chemical reactivity descriptors of compounds such as hardness, chemical potential, softness, electronegativity and electrophilicity index as well as local reactivity has been defined [35-37]. Pauling introduced the concept of electronegativity as the power of an atom in a compound to attract electrons. Hardness

(η), chemical potential (μ) electronegativity (χ) and softness are defined follows:

$$\eta = \frac{1}{2}(\partial\mu / \partial N)_{v(r)} = \frac{1}{2}(\partial^2 E / \partial N^2)_{v(r)}$$

$$\mu = (\partial E / \partial N)_{v(r)} = -\chi$$

where E and $v(r)$ are the electronic energy and external potential of an N-electron system respectively. Softness is a property of compound that measures the extent of chemical reactivity. It is the reciprocal of hardness

$$S = 1/2\eta$$

Using Koopman's theorem for closed-shell compounds η , μ and χ can be defined as,

$$\mu = -(IE + EA)/2 = (E_{N+1} - E_{N-1})/2 = -\chi$$

where A and I are the ionization potential and electron affinity of the compounds respectively. Electron affinity refers to the capability of ligand to accept precisely one electron from a donor. However, in many kinds of bonding viz. covalent hydrogen bonding, partial charge transfer takes places. Recently Parr and his colleagues have defined a new descriptor to quantify the global electrophilic power of the compound as electrophilicity index (ω), which defines a quantitative classification of global electrophilic nature of a compound. Parr and his colleagues have proposed electrophilicity index (ω) as a measure of energy lowering due to maximal electron flow between donor and acceptor. They defined electrophilicity index (ω) as follows:

$$\omega = \mu^2 / 2\eta$$

Electrophilicity index is one of the important quantum chemical descriptors in describing toxicity or biological activities of the molecules in the context of development of Quantitative Structure-Activity Relationship (QSAR) parlance. Quantitative Structure-Activity Relationship (QSAR) methodology is one of the most powerful tools for describing the relationships between biological activity and the physicochemical characteristics of molecules. The molecular descriptor is the final result of a logic and mathematical procedure which transforms chemical information encoded within a symbolic representation of a molecule into a useful number or the result of some standardized experiment. Many of the descriptors are based directly on the results of quantum-mechanical calculations or can be derived from the electronic wave function or electrostatic field of the molecule [38]. Since the electrophilicity index is a chemical reactivity descriptor and it has been used as appropriate descriptor of QSAR study. Recently the electrophilicity index has been used as a possible descriptor of biological activity confirming the fact that the electrophilicity properly quantifies the biological activity. A previous QSAR study made with Multiple Linear Regression and found that the HOMO and LUMO energies are the most important descriptors for describing the drug-receptor interaction of the molecules [39]. It has found that electrophilicity is sufficient enough to describe the toxicity of the molecule. The usefulness of this new reactivity quantity has recently demonstrated in understanding the toxicity of various pollutants in terms of their reactivity and site selectivity [40]. HOMO and LUMO related properties are presented in Table 6.

Table 6: Quantum chemical descriptors of mono-functionalized bisTTF **3(a-e)**

Parameters	3a	3b	3c	3d	3e
E_{HOMO} (eV)	-4.798	-4.835	-4.721	-4.772	-4.943
E_{LUMO} (eV)	-1.666	1.712	-1.905	-1.627	-1.657
ΔE_{gap} (eV)	3.132	6.548	2.816	3.144	3.285
IE (eV)	4.798	4.835	4.721	4.772	4.943
EA (eV)	1.666	-1.712	1.905	1.627	1.657
μ (eV)	-3.232	-1.562	-3.313	-3.200	-3.300
χ (eV)	3.232	1.562	3.313	3.200	3.300
η (eV)	1.566	3.274	1.408	1.572	1.643
S (eV)	0.319	0.153	0.355	0.318	0.304
ω (eV)	3.334	0.372	3.898	3.256	3.315

3.6. Local reactivity descriptors

The site selectivity of a chemical system cannot be studied using the global reactivity descriptors. For this purpose, appropriate local reactivity descriptors as Fukui function to describe the reactivity of an atom in a molecule are needed to be defined. The local reactivity descriptors [41-43] such as Fukui functions (f^+ , f^- , f^0) are calculated using the following equations as:

$$f^+ = [q(N+1) - q(N)], \text{ for nucleophilic attack,}$$

$$f^- = [q(N) - q(N-1)], \text{ for electrophilic attack,}$$

$$f^0 = [q(N+1) - q(N-1)]/2, \text{ for radical attack.}$$

In these equations, q is the atomic charge (evaluated from Mulliken population analysis, electrostatic derived charge, etc.) at the k_{th} atomic site is the neutral (N), anionic (N + 1) or cationic (N - 1) chemical species. Fukui functions for selected atomic sites in compounds **3(a-e)** are shown in Tables 7-9.

Table 7: Order of the reactive sites on compounds **3a** and **3b**

Compound 3a						Compound 3b					
Atom	24 C	28 C	2 C	16 C	27 C	Atom	27 C	24 C	2 C	16 C	3 C
f^+	0.024	0.020	0.019	0.017	0.014	f^+	0.050	0.028	0.018	0.016	0.009
Atom	16 C	2 C	4 C	27 C	23 C	Atom	16 C	2 C	4 C	23 C	27 C
f^-	0.056	0.020	0.013	0.009	0.006	f^-	0.059	0.020	0.014	0.006	0.006
Atom	0.036	0.020	0.013	0.013	0.012	Atom	16 C	27 C	2 C	24 C	23 C
f^0	16 C	2 C	24 C	28 C	27 C	f^0	0.038	0.028	0.019	0.016	0.006

Table 8: Order of the reactive sites on compounds **3c** and **3d**

Compound 3c						Compound 3d					
Atom	3 C	1 O	32 C	13 C	43 C	Atom	30 C	24 C	1 C	3 C	20 C
f^+	0.159	0.157	0.128	0.112	0.086	f^+	0.050	0.015	0.014	0.010	0.006
Atom	7 C	25 C	36 C	37 C	14 C	Atom	24 C	2 C	31 C	3 C	9 C
f^-	0.048	0.024	0.015	0.009	0.007	f^-	0.039	0.026	0.007	0.003	0.002
Atom	3 C	1 O	32 C	13 C	7 C	Atom	24 C	30 C	2 C	3 C	9 C
f^0	0.076	0.073	0.058	0.058	0.057	f^0	0.027	0.025	0.013	0.007	0.003

Table 9: Order of the reactive sites on compound **7e**

Compound 3e					
Atom	38 C	10 C	9 C	32 C	2 C
f^+	0.049	0.015	0.015	0.015	0.010
Atom	32 C	2 C	19 C	9 C	39 C
f^-	0.037	0.027	0.012	0.006	0.004
Atom	32 C	38 C	2 C	9 C	10 C
f^0	0.026	0.026	0.019	0.010	0.009

3.7. Natural bond orbital analysis (NBO)

The stabilization energies of the title compounds were computed by using second-order perturbation theory in order to investigate the intra and intermolecular interactions, interaction among bonds, conjugative interactions. For each donor NBO(i) (Natural Bond Orbital) and acceptor NBO(j), the stabilization energy E(2) associated with electron delocalization between donor and acceptor is estimated as [44,45].

$$E(2) = \Delta E_{ij} = q_i \frac{F^2(i,j)}{E_j - E_i}$$

where q_i is the donor orbital occupancy, E_i , E_j are diagonal elements (orbital energies) and F_{ij} is the off-diagonal NBO Fock matrix element.

The results of second-order perturbation theory analysis of the Kohn-Sham Matrix at B3LYP/6-31G (d,p) level of theory are presented in Tables 10-14.

Table 10: Second order perturbation theory analysis of Fock matrix on NBO of compound **3a**

Donor(i)	ED/e	Acceptor(j)	ED/e	E Kcal/mol	E(j)-E(i) a.u	F(i,j) a.u
LP(2)O20	1.79953	π^* C12-O21	0.27738	46.99	0.33	0.113
LP(2)O21	1.84092	δ^* C12-O20	0.10457	33.49	0.62	0.131
LP(2)S15	1.73305	π^* C13-C25	0.25974	25.61	0.26	0.072
LP(2)S5	1.76194	π^* C3-C4	0.23117	23.11	0.26	0.069
LP(2)S14	1.77661	π^* C13-C25	0.25974	21.12	0.25	0.065
LP(2)S6	1.78107	π^* C3-C4	0.23117	20.76	0.26	0.066
LP(2)S19	1.79602	π^* C27-C28	0.36707	19.58	0.24	0.063
LP(2)S8	1.79987	π^* C23-C24	0.36681	19.42	0.24	0.063
LP(2)S7	1.80019	π^* C23-C24	0.36681	19.39	0.24	0.063
LP(2)S18	1.79869	π^* C27-C28	0.36707	19.30	0.24	0.063
π C13-C25	1.90090	π^* C12-O21	0.27738	18.46	0.31	0.070
LP(2)O21	1.84092	δ^* C12-C13	0.06571	18.36	0.70	0.103
LP(2)S37	1.85590	π^* C27-C28	0.36707	17.41	0.24	0.061
LP(2)S30	1.85679	π^* C23-C24	0.36681	17.30	0.24	0.061
LP(2)S14	1.77661	π^* C16-C17	0.37904	17.25	0.25	0.062
LP(2)S6	1.78107	π^* C1-C2	0.38033	16.95	0.26	0.062
LP(2)S5	1.76194	π^* C1-C2	0.38033	16.87	0.26	0.061
LP(2)S15	1.73305	π^* C16-C17	0.37904	16.30	0.26	0.060
LP(2)S18	1.79869	π^* C16-C17	0.37904	13.23	0.25	0.054
LP(2)S19	1.79602	π^* C16-C17	0.37904	13.16	0.25	0.054

Table 11: Second order perturbation theory analysis of Fock matrix on NBO of compound **3b**

Donor(i)	ED/e	Acceptor(j)	ED/e	E Kcal/mol	E(j)-E(i) a.u	F(i,j) a.u
LP(2)O20	1.79971	π^* C12-O21	0.27779	47.06	0.33	0.113
LP(2)O21	1.84103	δ^* C12-O20	0.10462	33.49	0.62	0.131
LP(2)S15	1.73486	π^* C13-C25	0.25983	25.63	0.26	0.072
LP(2)S5	1.76231	π^* C3-C4	0.23109	23.08	0.26	0.069
LP(2)S14	1.77933	π^* C13-C25	0.25983	21.11	0.25	0.065
LP(2)S6	1.78100	π^* C3-C4	0.23109	20.79	0.26	0.066
LP(2)S8	1.80003	π^* C23-C24	0.36694	19.39	0.24	0.063
LP(2)S19	1.78788	π^* C27-C28	0.31178	19.36	0.25	0.063
LP(2)S7	1.80040	π^* C23-C24	0.36694	19.35	0.24	0.063
LP(2)S18	1.79148	π^* C27-C28	0.31178	18.98	0.25	0.063
π C13-C25	1.90102	π^* C12-O21	0.27779	18.48	0.31	0.070
LP(2)O21	1.84103	δ^* C12-C13	0.06562	18.34	0.70	0.103
LP(2)S30	1.85645	π^* C23-C24	0.36694	17.48	0.24	0.061
LP(2)S14	1.77933	π^* C16-C17	0.37934	17.10	0.26	0.061
LP(2)S6	1.78100	π^* C1-C2	0.38029	16.94	0.26	0.062
LP(2)S5	1.76231	π^* C1-C2	0.38029	16.84	0.26	0.061
LP(2)S15	1.73486	π^* C16-C17	0.37934	16.18	0.27	0.06
LP(2)S19	1.78788	π^* C16-C17	0.37934	13.79	0.25	0.055
LP(2)S18	1.79148	π^* C16-C17	0.37934	13.71	0.26	0.055
LP(2)S8	1.80003	π^* C1-C2	0.38029	12.84	0.26	0.054

Table 12: Second order perturbation theory analysis of Fock matrix on NBO of compound **3c**

Donor(i)	ED/e	Acceptor(j)	ED/e	E Kcal/mol	E(j)-E(i) a.u	F(i,j) a.u
$\pi^*C43-C50$	0.40147	$\pi^*C46-C48$	0.34645	204.23	0.02	0.083
$\pi^*C42-C44$	0.40165	$\pi^*C46-C48$	0.34645	203.18	0.02	0.083
LP(2)O1	1.78787	π^*C2-O4	0.26951	42.78	0.34	0.109
LP(2)O4	1.83434	δ^*O1-C2	0.11477	36.52	0.61	0.135
LP(2)S8	1.73259	π^*C3-C6	0.26286	25.91	0.25	0.073
$\pi C46-C48$	1.66399	$\pi^*C42-C44$	0.40165	21.65	0.26	0.069
$\pi C46-C48$	1.66399	$\pi^*C43-C50$	0.40147	21.64	0.26	0.069
$\pi C26-C28$	1.67780	$\pi^*C25-C27$	0.37240	21.45	0.28	0.070
LP(2)S5	1.78027	π^*C3-C6	0.26286	21.10	0.24	0.065
$\pi C25-C27$	1.64899	$\pi^*C30-C32$	0.37522	20.65	0.29	0.070
$\pi C30-C32$	1.64612	$\pi^*C26-C28$	0.32020	20.54	0.28	0.068
$\pi C30-C32$	1.64612	$\pi^*C25-C27$	0.37240	20.44	0.27	0.067
LP(2)S38	1.78315	$\pi^*C37-C52$	0.24718	19.45	0.27	0.066
LP(2)S12	1.78711	$\pi^*C13-C14$	0.31289	19.33	0.25	0.063
$\pi C25-C27$	1.64899	$\pi^*C26-C28$	0.32020	19.31	0.29	0.068
LP(2)S11	1.79087	$\pi^*C13-C14$	0.31289	18.95	0.25	0.063
$\pi C43-C50$	1.68329	$\pi^*C42-C44$	0.40165	18.72	0.28	0.066
$\pi C42-C44$	1.68350	$\pi^*C43-C50$	0.40147	18.71	0.28	0.066
$\pi C26-C28$	1.67780	$\pi^*C30-C32$	0.37522	18.64	0.28	0.066
$\pi C3-C6$	1.89840	π^*C2-O4	0.26951	18.50	0.31	0.070

Table 13: Second order perturbation theory analysis of Fock matrix on NBO of compound **3d**

Donor(i)	ED/e	Acceptor(j)	ED/e	E Kcal/mol	E(j)-E(i) a.u	F(i,j) a.u
LP(2)O18	1.80391	$\pi^*C19-O21$	0.27379	47.07	0.33	0.114
LP(2)O21	1.84121	$\delta^*O18-C19$	0.10285	33.96	0.63	0.132
LP(2)S25	1.73800	$\pi^*C20-C23$	0.25889	25.34	0.26	0.072
LP(2)S6	1.77855	π^*C3-C4	0.31286	21.64	0.23	0.065
LP(2)S22	1.77796	$\pi^*C20-C23$	0.25889	21.25	0.25	0.065
LP(2)S5	1.78613	π^*C3-C4	0.31286	20.71	0.23	0.064
LP(2)S8	1.78918	$\pi^*C9-C10$	0.23221	19.66	0.27	0.066
LP(2)S7	1.79030	$\pi^*C9-C10$	0.23221	19.55	0.27	0.066
LP(2)S29	1.78831	$\pi^*C30-C31$	0.31265	19.33	0.25	0.063
LP(2)S28	1.79189	$\pi^*C30-C31$	0.31265	18.95	0.25	0.063
LP(2)O21	1.84121	$\delta^*C19-C20$	0.06706	18.75	0.69	0.104
$\pi C20-C23$	1.90481	$\pi^*C19-O21$	0.27379	17.91	0.31	0.070
LP(2)S22	1.77796	$\pi^*C24-C27$	0.37890	17.06	0.25	0.061
LP(2)S8	1.78918	π^*C1-C2	0.38191	16.98	0.26	0.062
LP(2)S7	1.79030	π^*C1-C2	0.38191	16.93	0.26	0.062
LP(2)S25	1.73800	$\pi^*C24-C27$	0.37890	16.10	0.26	0.060
LP(2)S29	1.78831	$\pi^*C24-C27$	0.37890	13.68	0.25	0.055
LP(2)S28	1.79189	$\pi^*C24-C27$	0.37890	13.60	0.26	0.055
LP(2)S6	1.77855	π^*C1-C2	0.38191	13.50	0.26	0.055
LP(2)S5	1.78613	π^*C1-C2	0.38191	13.22	0.26	0.055

Table 14: Second order perturbation theory analysis of Fock matrix on NBO of compound **3e**

Donor(i)	ED/e	Acceptor(j)	ED/e	E Kcal/mol	E(j)-E(i) a.u	F(i,j) a.u
LP(2)O26	1.80464	π^* C27-O29	0.27348	46.89	0.33	0.114
LP(2)O29	1.84110	δ^* O26-C27	0.10313	34.05	0.63	0.132
LP(2)S33	1.73746	π^* C28-C31	0.25938	25.42	0.26	0.072
LP(2)S6	1.76857	π^* C3-C4	0.31247	21.82	0.23	0.065
LP(2)S30	1.77822	π^* C28-C31	0.25938	21.25	0.25	0.065
LP(2)S5	1.77589	π^* C3-C4	0.31247	20.90	0.23	0.064
LP(2)S8	1.79305	π^* C9-C10	0.36710	19.61	0.24	0.063
LP(2)S7	1.79465	π^* C9-C10	0.36710	19.47	0.24	0.063
LP(2)S37	1.78805	π^* C38-C39	0.31280	19.35	0.25	0.063
LP(2)S36	1.79211	π^* C38-C39	0.31280	18.91	0.25	0.063
LP(2)O29	1.84110	δ^* C27-C28	0.06701	18.76	0.69	0.104
π C28-C31	1.90449	π^* C27-O29	0.27348	17.96	0.31	0.070
LP(2)S12	1.85693	π^* C9-C10	0.36710	17.29	0.24	0.061
LP(2)S30	1.77822	π^* C32-C35	0.37896	17.06	0.26	0.061
LP(2)S33	1.73746	π^* C32-C35	0.37896	16.11	0.27	0.06
LP(2)S6	1.76857	π^* C1-C2	0.37299	15.01	0.26	0.058
LP(2)S5	1.77589	π^* C1-C2	0.37299	14.74	0.26	0.057
LP(2)S37	1.78805	π^* C32-C35	0.37896	13.69	0.25	0.055
LP(2)S36	1.79211	π^* C32-C35	0.37896	13.63	0.26	0.055
LP(2)S8	1.79305	π^* C1-C2	0.37299	13.52	0.26	0.055

3.8. Nonlinear optical properties (NLO)

Non-linear optics deals with the interaction of applied electromagnetic fields in various materials to generate new electromagnetic fields, altered in wave number, phase or other physical properties [46]. Organic molecules able to manipulate photonic signals efficiently are of importance in technologies such as optical communication, optical computing and dynamic image processing [47,48]. In this context the first hyperpolarizability of the title compounds are also calculated in the present study. The first hyperpolarizability of these novel molecular systems is calculated using DFT method based on the finite field approach. In the presence of an applied electric field, the energy of a system is a function of the electric field. First hyperpolarizability is a third rank tensor that can be described by a $3 \times 3 \times 3$ matrix. The 27 components of the 3D matrix can be reduced to 10 components due to the Kleinman symmetry [49]. The components of β are defined as the coefficients in the Taylor series expansion of the energy in the external electric field. When the electric field is weak and homogeneous, this expansion becomes

$$E = E^0 - \mu_i F_i - 1/2 \alpha_{ij} F_i F_j - 1/6 \beta_{ijk} F_i F_j F_k + \dots$$

Where E^0 is the energy of the unperturbed molecules, F_i is the field at the origin and μ_i , α_{ij} , β_{ijk} are the components of dipole moment, polarizability, and first hyperpolarizability, respectively. The total static dipole moment (μ_0), anisotropy of the polarizability (α_0), mean polarizability ($\Delta\alpha$) and the total first hyperpolarizability (β_0) using (x, y, z) components are defined as [50]:

$$\mu_{tot} = [\mu_x^2 + \mu_y^2 + \mu_z^2]^{1/2}$$

$$\alpha = (\alpha_{xx} + \alpha_{yy} + \alpha_{zz})/3$$

$$\Delta\alpha = 2^{-1/2} [(\alpha_{xx} - \alpha_{yy})^2 + (\alpha_{yy} - \alpha_{zz})^2 + (\alpha_{zz} - \alpha_{xx})^2 + 6\alpha_{xz}^2 + 6\alpha_{xy}^2 + 6\alpha_{yz}^2]^{1/2}$$

$$\beta_{tot} = (\beta_x^2 + \beta_y^2 + \beta_z^2)^{1/2}$$

$$\beta_x = \beta_{xxx} + \beta_{xyx} + \beta_{xzx}$$

$$\beta_y = \beta_{yyy} + \beta_{xyy} + \beta_{yzy}$$

$$\beta_z = \beta_{zzz} + \beta_{xxz} + \beta_{yzz}$$

The total molecular dipole moment and first order hyperpolarizability are depicted in Table 15. The calculated hyperpolarizability of the title compounds is 35 times that of the standard NLO material urea (0.13×10^{-30} esu) [51]. We conclude that the title compound is an attractive object for future studies of nonlinear optical properties.

Table 15: The dipole moments μ (D), polarizability α , the anisotropy of the polarizability $\Delta\alpha$ (esu), and the first hyperpolarizability β (esu) of mono-functionalized bisTTF **3(a-e)**

Parameters	3a	3b	3c	3d	3e
β_{xxx}	-209.359	-778.587	-580.589	1118.394	1189.897
β_{yyy}	8.506	-31.028	-1.019	53.188	68.992
β_{zzz}	26.877	24.484	14.619	70.880	48.589
β_{xyy}	70.081	-60.440	16.835	-30.674	-62.454
β_{xxy}	-309.639	-352.577	-137.981	93.809	94.802
β_{xxz}	-367.971	-41.763	152.570	146.644	-13.529
β_{xzz}	-14.926	77.194	101.103	-0.310	18.116
β_{yzz}	6.951	-16.369	2.679	18.449	24.573
β_{yyz}	1.798	-30.645	26.160	6.765	16.505
β_{xvz}	28.556	-23.692	-3.285	64.776	86.647
$\beta_{tot}(\text{esu}) \times 10^{-33}$	4232.154	3745.054	4644.659	10498.923	11311.488
μ_x	-0.301	-4.020	-0.684	5.192	4.415
μ_y	-2.455	-3.153	-1.715	3.733	4.096
μ_z	-0.627	-1.399	1.925	2.083	0.576
$\mu_{tot}(\text{D})$	2.551	5.298	2.668	6.725	6.050
α_{xx}	-175.240	-265.272	-278.053	-230.246	-255.669
α_{yy}	-268.402	-246.876	-268.195	-281.183	-306.831
α_{zz}	-264.279	-262.969	-290.406	-277.582	-302.777
α_{xy}	-11.554	8.443	4.701	-18.614	-26.527
α_{xz}	6.460	6.237	39.426	-21.237	-36.121
α_{yz}	7.265	-1.468	2.619	7.068	8.736
$\alpha(\text{esu}) \times 10^{-24}$	-34.971	-38.291	-41.331	-38.977	-42.745
$\Delta\alpha(\text{esu}) \times 10^{-24}$	14.056	3.744	10.606	10.444	13.808

4. Conclusion

From the whole of the results presented in this contribution it has been clearly demonstrated that the sites of interaction of the title compounds **3(a-e)** can be predicted by using DFT-based reactivity descriptors such as the hardness, softness, and electrophilicity, as well as Fukui-function calculations. These descriptors were used in the characterization and successful description of the preferred reactive sites and provide a firm explanation for the reactivity of the mono-functionalized bis-tetrathiafulvalenes. NBO and NLO analysis reveals that the some important intramolecular charge transfer can induce large nonlinearity to the title molecules and the intramolecular conjugative interaction around the tetrathiafulvalene core can induce the large conductivity in the compounds. Finally we hope that these consequences will be of assistance in the quest of the experimental and theoretical evidence for the title compounds in molecular bindings.

Acknowledgments

This work was generously supported by the (General Directorate for Scientific Research and Technological Development, DGRS-DT) and Algerian Ministry of Scientific Research.

References

- [1] Wudl F, Wobschall D, Hufnagel E J. Electrical conductivity by the bis(1,3-dithiole)-bis(1,3-dithiolium) system. *J. Am. Chem. Soc.* 94: 670-672; 1972.
- [2] Ferraris J, Cowan D O, Walatka VV, Perlstein JH. Electron transfer in a new highly conducting donor-acceptor complex. *J. Am. Chem. Soc.* 95: 948-949; 1973.
- [3] Torrent MM, Durkut M, Hadley P, Ribas X, Rovira C. High Mobility of Dithiophene-Tetrathiafulvalene Single-Crystal Organic Field Effect Transistors. *J. Am. Chem. Soc.* 126: 984-985; 2004.
- [4] Bendikov M, Wudl F, Perepichka DF. Tetrathiafulvalenes, Oligoacenes, and Their Buckminsterfullerene Derivatives: The Brick and Mortar of Organic Electronics. *Chem. Rev.* 104: 4891-4945; 2004.
- [5] Hou Y, Chen Y, Liu Q, Yang M, Wan X, Yin S, Yu A. A Novel Tetrathiafulvalene- (TTF-) Fused Poly(aryleneethynylene) with an Acceptor Main Chain and Donor Side Chains: Intramolecular Charge Transfer (CT), Stacking Structure, and Photovoltaic Property. *Macromolecules.* 41: 3114-3119; 2008.
- [6] Kanato H, Narutaki M, Takimiya K, Otsubo T, Harima Y. Synthesis and Photovoltaic Properties of Tetrathiafulvalene-Oligothiophene-Fullerene Triads. *Chem. Lett.* 35: 668-669; 2006.
- [7] Yamada J, Akutsu H, Nishikawa H, Kikuchi K. New trends in the synthesis of π -electron donors for molecular conductors and superconductors. *Chem. Rev.* 104: 5057-5083; 2004.
- [8] Mori H. Materials Viewpoint of Organic Superconductors. *J. Phys. Soc. Jpn.* 75: 051003; 2006.
- [9] Mulliken RS. Molecular Compounds and their Spectra. *J. Am. Chem. Soc.* 74: 811-824; 1952.
- [10] Kobayashi A, Fujiwara E, Kobayashi H. Single-Component Molecular Metals with Extended-TTF Dithiolate Ligands. *Chem. Rev.* 104: 5243-5264; 2004.
- [11] Zhang Y, Guo ZJ, You XZ. Hydrolysis Theory for Cisplatin and Its Analogues Based on Density

- Functional Studies. *J. Am. Chem. Soc.* 123: 9378-9387; 2001.
- [12] Proft FD, Geerlings P. Conceptual and Computational DFT in the Study of Aromaticity. *Chem. Rev.* 101: 1451-1464; 2001.
- [13] Fitzgerald G, Andzelm J. Chemical applications of density functional theory: comparison to experiment, Hartree-Fock, and perturbation theory. *J. Phys. Chem.* 95: 10531-10534; 1991.
- [14] Tanak H. Crystal Structure, Spectroscopy, and Quantum Chemical. *Int. J. Quant. Chem.* 112: 2392-2402; 2012.
- [15] Gupte SS, Marcano A, Pradhan RD, Desai CF, Melikechi J. Pump-probe thermal lens near-infrared spectroscopy and Z-scan study of zinc (tris) thiourea sulfate. *J. Appl. Phys.* 89: 4939-4943; 2001.
- [16] Karna SP. (Ed.), *Electronic and Nonlinear Optical Materials: The Role of Theory and Modeling*. *J. Phys. Chem. A.* 104: 4671-4673; 2000.
- [17] Carcel C, Kaboub L, Gouasmia AK, Fabre JM. Synthesis and redox properties of several new oligoTTF containing functional spacer. *Synthetic Metals.* 156: 1271-1279; 2006.
- [18] Binet L, Fabre JM. Synthesis of New Functionalized π -Electron Donors: Primary Hydroxy and Primary Amino Multisulfur Tetrathiafulvalenes. *Synthesis.* 10: 1179 -1184; 1997.
- [19] Blanchard P, Salle M, Duguay G, Jubault M, Gorgues A. A simple 1,5 \rightarrow 1,3-diketone rearrangement. *Tetrahedron Lett.* 33: 2685-2688; 1992.
- [20] Moore AJ, Bryce MR, Batsanov AS, Cole JC, Howard JAK. Functionalised Trimethyltetrathiafulvalene (TriMe-TTF) Derivatives via Reactions of Trimethyltetrathiafulvalenyllithium with Electrophiles: X-ray Crystal Structures of Benzoyl-TriMe-TTF and Benzoylthio-TriMe-TTF. *Synthesis.* 6: 675-682; 1995.
- [21] Heuze K, Fourmigue M, Batail P. The crystal chemistry of amide-functionalized ethylenedithio-tetrathiafulvalenes: EDT-TTF-CONRR' (R, R' = H, Me). *J. Mater. Chem.* 9: 2373-2379; 1999.
- [22] Heuze K, Meziere C, Fourmigue M, Batail P, Coulon C, Canadell E, Auban-Senzier P, Jerome D. Directing the Structures and Collective Electronic Properties of Organic Conductors: The Interplay of π -Overlap Interactions and Hydrogen Bonds. *Chem. Eur. J.* 5: 2971; 1999.
- [23] Heuze K, Fourmigue M, Batail P, Canadell E, Auban-Senzier P. An Efficient, Redox-Enhanced Pair of Hydrogen-Bond Tweezers for Chloride Anion Recognition, a Key Synthon in the Construction of a Novel Type of Organic Metal based on the Secondary Amide-Functionalized Ethylenedithiotetrathiafulvalene, β -(EDT-TTF-CONHMe)₂[Cl·H₂O]. *Chem. Mater.* 12: 1898-1904; 2000.
- [24] Politzer P, Laurence PR, Jayasuriya K. Molecular electrostatic potentials: an effective tool for the elucidation of biochemical phenomena, in: J. McKinney (Ed.), *Structure Activity Correlation in Mechanism Studies and Predictive Toxicology*, *Environ. Health Perspect.* 61: 191-202; 1985.
- [25] Politzer P, Lane P. A computational study of some nitrofluoromethanes. *Struct. Chem.* 1: 159-164; 1990.
- [26] Scrocco E., Tomasi J., *Electronic Molecular Structure, Reactivity and Intermolecular Forces: An Euristic Interpretation by Means of Electrostatic Molecular Potentials*. *Adv. Quantum Chem.* 11: 115-193; 1979.
- [27] Luque FJ, Lopez JM, Orozco M. Perspective on "electrostatic interactions of a solute with a

- continuum. A direct utilization of ab initio molecular potentials for the prevision of solvent effects”, *Theor. Chem. Acc.* 103: 343-345; 2000.
- [28] Politzer P, Truhlar DG. *Chemical Applications of Atomic and Molecular Electrostatic Potentials*, Plenum Press, New York, 1981.
- [29] Bader RFW. A quantum theory of molecular structure and its applications, *Chem. Rev.* 91: 893-928; 1990.
- [30] Murray JS, Sen K. *Molecular Electrostatic Potentials. Concepts and Applications*, Elsevier, Amsterdam, 1996.
- [31] Seminario JM. *Recent Development and Applications of Modern Density Functional Theory*. Elsevier. 4: 800-806; 1996.
- [32] Yesilkayanak T, Binzet G, Mehmet Emen F, Florke U, Kulcu N, Arslan H. *Eur. J. Chem.* 1: 1-5; 2010.
- [33] Belletete M., Morin J.F., Leclerc M., Durocher G., A Theoretical, Spectroscopic, and Photophysical Study of 2,7-Carbazolenevinylene-Based Conjugated Derivatives. *J. Phys. Chem. A.* 109: 6953-6959; 2005.
- [34] Zhenming D, Heping S, Yufang L, Diansheng L, Bo L. Experimental and theoretical study of 10-methoxy-2-phenylbenzo[h]quinoline. *Spectrochim. Acta A.* 78: 1143-1148; 2011.
- [35] Parr RG, Szentpaly LV, Liu SJ. *Electrophilicity Index*. *Am. Chem. Soc.* 121: 1922-1924; 1999.
- [36] Chattraj PK, Maiti B, Sarbar UJ. *Philicity: A Unified Treatment of Chemical Reactivity and Selectivity*. *J. Phys. Chem. A.* 107: 4973-4975; 2003.
- [37] Parr RG, Donnelly RA, Levy M, Palke WE. *Am. Chem. Soc.* 68: 3801-3807; 1978.
- [38] Puzyn T, Leszczynski J, Cronin MTD. *Recent Advances in QSAR Studies*, Springer, New York, NY, USA, 2010. 30-41.
- [39] Garrido AP, Helguera AM, Guillén AA, Cordeiro MNDS, Escudero AG. Convenient QSAR model for predicting the complexation of structurally diverse compounds with β -cyclodextrins. *Bioorgan. Med. Chem.* 17: 896-904; 2009.
- [40] Parthasarathi R, Padmanabhan J, Subramanian V, Sarkar U, Maiti B, Chattraj PK. Toxicity analysis of benzidine through chemical reactivity and selectivity profiles: a DFT approach. *Int. Electron. J. Mol. Des.* 2: 798-813; 2003.
- [41] Srivastava A, Rawat P, Tandon P, Singh RN. A computational study on conformational geometries, chemical reactivity and inhibitor property of an alkaloid bicuculline with γ -aminobutyric acid (GABA) by DFT. *Comp. Theor. Chem.* 993: 80-89; 2012.
- [42] Singh RN, Baboo V, Rawat P, Kumar A, Verma D. Molecular structure, spectral studies, intra and intermolecular interactions analyses in a novel ethyl 4-[3-(2-chloro-phenyl)-acryloyl]-3,5-dimethyl-1H-pyrrole-2-carboxylate and its dimer: A combined DFT and AIM approach. *Spectrochim. Acta Part A.* 94: 288-301; 2012.
- [43] Singh RN, Kumar A, Tiwari RK, Rawat P, Manohar R. Synthesis, molecular structure, and spectral analyses of ethyl-4-[(2,4-dinitrophenyl)-hydrazonomethyl]-3,5-dimethyl-1H-pyrrole-2-carboxylate. *Struct. Chem.* 24: 713-724; 2013.
- [44] Schwenke DW, Truhlar DG. Systematic study of basis set superposition errors in the calculated interaction energy of two HF molecules. *J. Chem. Phys.* 82: 2418-2426; 1985.

- [45] Gutowski M, RakPawel J, Blazejowski D. Theoretical Studies on the Geometry, Thermochemistry, Vibrational Spectroscopy, and Charge Distribution in TiX_6 - ($X = F, Cl, Br, I$). Coulombic Energy in hexahalogenotitanate Lattices. *J. Chem. Phys.* 98: 6280-6286; 1994.
- [46] Shen YR. *The Principles of Non-linear Optics*, Wiley, New York, 1984.
- [47] Eaton DF. Nonlinear optical materials. *Science*. 253: 281-287; 1991.
- [48] Kolinsky PV. New materials and their characterization for photonic device applications. *Opt. Eng.* 31: 1676-1684; 1992.
- [49] Kleinman DA. Nonlinear Dielectric Polarization in Optical Media. *Phys. Rev.* 126: 1977-1979; 1962.
- [50] Karna SP, Prasad PN, Dupuis M. Nonlinear optical properties of *p*-nitroaniline: an ab initio time-dependent coupled perturbed Hartree-Fock study. *J. Chem. Phys.* 94: 1171-1181; 1991.
- [51] Adant C, Dupuis M, Bredas JL. Ab initio study of the nonlinear optical properties of urea: Electron correlation and dispersion effects. *Int. J. Quantum Chem.* 56: 497-507; 2004.